Charge State of Fast Heavy Ions in a Hydrogen Plasma

K.-G. Dietrich,[1] D. H. H. Hoffmann,[1] E. Boggasch,[2] J. Jacoby,[2] H. Wahl,[2] M. Elfers,[3] C. R. Haas,[3] V. P. Dubenkov,[4] and A. A. Golubev[4]

[1]*Gesellschaft für Schwerionenforschung (GSI), Postfach 110552, D-6100 Darmstadt, Germany*
[2]*Max-Planck-Institut für Quantenoptik (MPQ), D-8046 Garching, Germany*
[3]*Lehrstuhl für Lasertechnik, Rheinisch-Westfälische Technische Hochschule Aachen, D-5100 Aachen, Germany*
[4]*Institute for Theoretical and Experimental Physics, 117259 Moscow, Russia*

(Received 27 February 1992)

We report the first charge-state measurements of fast heavy ions passing through a plasma target. The projectiles were ^{40}Ar ions at an energy of 4.8 MeV/amu and ^{129}Xe ions at an energy of 5.9 MeV/amu. The target was a 20-cm-long Z pinch discharge which provided fully ionized hydrogen plasma with free electron densities up to 1.5×10^{19} cm^{-3}. The measured charge-state distributions are in excellent agreement with theoretical calculations. For Xe ions an increase of the ion charge state in plasma over the charge state in cold gas was observed.

PACS numbers: 34.50.Bw, 52.20.Hv, 52.40.Mj

Ion-beam-induced inertial confinement fusion (ICF) is today regarded as an attractive alternative to magnetic confinement fusion (MCF) schemes. A detailed modeling of the beam energy coupling to the ablator regime of a fusion pellet depends strongly on the precise knowledge of the energy deposition process of heavy ions in ionized matter. Since the energy deposition process is strongly dependent on the charge state of the projectiles, the charge state of fast heavy ions in a plasma is a key issue when intense heavy-ion beams are used to heat small samples of matter to high temperatures [1].

In a standard model approach [2] the energy loss dE/dx of fast heavy ions in fully ionized plasma is calculated in terms of a modified Bethe formula,

$$\frac{dE}{dx} = -4\pi n_e \frac{Z_{\text{eff}}^2 e^4}{mv^2} \ln\frac{2mv^2}{\hbar\omega_p}, \qquad (1)$$

where n_e, $Z_{\text{eff}}e$, m, and v are free electron density, effective ion charge, electron rest mass, and ion velocity. Compared to the usual Bethe formula for cold matter the mean ionization potential of the target (commonly denoted at $\bar{I}$) is replaced by the excitation energy of a plasma wave $\hbar\omega_p$ in the logarithm (so-called Coulomb logarithm). Typically $\hbar\omega_p$ is much smaller than $\bar{I}$ (compare $\hbar\omega_p = 0.083$ eV at $n_e = 5\times10^{18}$ cm^{-18} to $\bar{I} = 19$ eV for molecular hydrogen). Thus the Coulomb logarithm in plasma is larger than in cold matter, leading to a higher plasma stopping power. As Eq. (1) illustrates, the energy loss of a fast heavy ion depends quadratically on its effective charge and a precise modeling of the ion charge in plasma is crucial for a correct calculation of the energy deposition.

Whereas for cold targets the problem of the charge state of heavy ions passing through matter has been studied for many decades theoretically as well as experimentally [3,4], for plasma targets up to now the work has been restricted to theory only. The first stimulating calculations were carried out by Nardi and Zinamon [5], who predicted an increase of the effective charge in fully ionized plasma compared to cold gas. The reason is that for a fast heavy ion the cross section for the capture of a free electron is much smaller than for the capture of a bound electron. As a result, the equilibrium ion charge state in plasma, which is determined by the balance of electron loss and electron capture processes, can exceed the cold-gas value considerably.

The results of Ref. [5] were corroborated by calculations of Peter, Arnold, and Meyer-ter-Vehn [6] who particularly emphasized the importance of dielectronic recombination (DR). It was predicted that due to its resonant character DR in many cases is the dominant electron capture process in plasma and thus determines the equilibrium projectile charge. An excellent comprehensive treatment of the theory of energy loss and charge state of fast heavy ions has been published recently [7,8].

The experiments investigating the interaction of fast ions with plasma so far were limited to measurements of the ion energy loss. An enhanced stopping power of a plasma for fast ions was first observed for deuterons and protons [9,10]. Later, systematic energy-loss measurements of heavy ions in hydrogen plasmas created in gas discharges showed an enhancement of the plasma stopping power of factors 2 to 2.5 compared to cold hydrogen gas [2,11,12]. This effect was mainly attributed to the higher Coulomb logarithm in plasma. Recently, energy-loss measurements in a Z pinch plasma showed enhancement factors up to 3 [13,14], which gave the first evidence for an increase of the ion charge state in plasma. However, the separation of the two effects of higher Coulomb logarithm and higher charge state from energy-loss data alone always bears some ambiguity.

We have therefore performed a first experiment to measure directly the charge-state distribution of heavy ions after passing through a plasma target. The experimental setup as installed at the UNILAC accelerator at GSI is displayed in Fig. 1. The projectiles were ^{40}Ar at 4.8 MeV/amu and ^{129}Xe at 5.9 MeV/amu. Stripper foils of different thicknesses allowed us to vary the projectile charge state before the projectile entered the plasma target.

We developed a Monte Carlo code to simulate energy-loss and charge-exchange processes of heavy ions in-

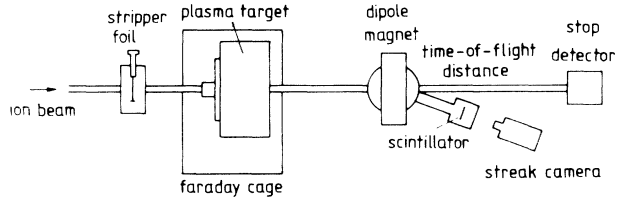

FIG. 1. Experimental setup.

teracting with ionized matter. This code is entirely based on Ref. [7] for the modeling of charge-exchange cross sections. This calculation predicts a different effect for the two projectiles. For Ar at 4.8 MeV/amu the effective charge observed under the conditions of our plasma target should be equal to that in cold gas of equal density. For Xe at 5.9 MeV/amu the effective charge in the plasma target should exceed the cold-gas value. We point out already here that exactly this behavior was found in the experiment.

The key element of the setup is the plasma target, a Z pinch device, which has been developed especially for the purpose of our beam-plasma experiments [15,16]. In eight capacitors with a total capacity of 4 μF, an energy of 2.1 kJ is stored at a typical voltage of 32.5 kV. The discharge vessel consists of a cylindrical quartz tube with a length of 20 cm and an inner diameter of 10.4 cm and copper electrodes at both ends. It is filled with hydrogen gas at a typical pressure of 2.5 mbar. The target is integrated into the vacuum system of the beam line using a differential pumping system. The beam passes through the target on the axis of symmetry through small apertures 3 mm in diameter and 40 mm in length in the electrodes. Tests with different gas pressures have proven that the differential pumping system is powerful enough to avoid charge-exchange processes of the ions by collisions with residual gas outside the tube. A rough estimate for the end zones ($\bar{p}=1.25$ mbar, $l=40$ mm) yields an integrated electron density of 2.5×10^{17} cm^{-2} and a capture cross section of $\sigma_{0c}=1.3\times10^{-20}$ cm^2 for bound electrons to be compared to 3×10^{20} cm^{-2} for the free-electron line density and a capture cross section $\sigma_{ic}=4.6\times10^{-22}$ cm^2 for free electrons. The ratio $n_e\sigma_{0c}l_0/n_e\sigma_{ic}l_i$ is approximately 0.02 and therefore end-zone effects changing the charge state due to bound electron capture can be neglected. Moreover, spectroscopic investigations of the end zones show that they are filled with plasma rather than cold gas during the pinch phase. The Z pinch device together with the differential pumping system is placed inside a Faraday cage to shield detectors and cameras against the high level of electromagnetic noise associated with the discharge.

The Z pinch plasma exhibits a strongly dynamical behavior. In the compression phase the azimuthal magnetic field accelerates the plasma cylinder onto the axis where after 1.2 μs a hot and dense pinched plasma column is formed. The kinetic pressure then exceeds the magnetic pressure and the column expands again. The resulting temporal evolution of the plasma density on the beam axis is displayed in the upper part of Fig. 2. It has been determined by on-axis interferometry [16] for $n_e\leq3\times10^{18}$ cm^{-3} and by the measured heavy-ion energy loss for the higher densities. The density rises steeply when the shock front reaches the axis and then gradually decreases as the plasma expands again. Side-on framing images have proven a very good stability and reproducibility of the whole compression and expansion process. The maximum density is $n_e=(1.5\pm0.2)\times10^{19}$ cm^{-3} which is more than 100 times the initial gas density.

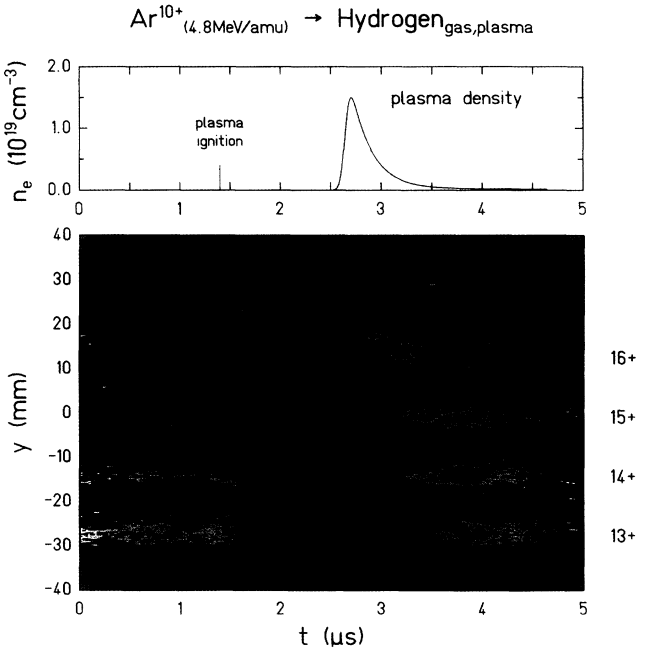

FIG. 2. Plasma density on the beam axis vs time (top) and streak image of the charge-state distribution of Ar ions after passing through the plasma target (false color image, bottom).

Plasma temperature measurements by spectroscopy of the emitted plasma light yield maximum temperatures of more than 6 eV and a degree of ionization of more than 99%. Ionization remains higher than 99% during the first microsecond of the expansion process while the plasma density decreases by 2 orders of magnitude. Full target ionization is a necessary prerequisite for this experiment. All presented charge-state data were taken under these conditions in the phase of plasma expansion and in a density region below 10^{19} cm^{-3}.

After passing through the plasma target the energy loss and the charge-state distribution of the ion beam are measured by two different techniques.

A 12-m-long straight beam line is used for a time-of-flight measurement of the ion energy loss. The procedure is the same as described in [12] and a detailed presentation of the results will be published in a forthcoming paper.

The charge-state distribution is analyzed by means of a novel detector system consisting of a magnetic dipole, a scintillator screen, and a fast streak camera. In the di-

pole the ions of different charge states are separated and deflected onto a sheet of plastic scintillator where each charge state produces a luminous beam spot. With a system consisting of a streak camera and a charge-coupled-device (CCD) camera we record the pattern on the scintillator while the plasma target is fired. By this means we are able to detect a time-resolved charge-state distribution of the heavy ions that have traversed the plasma target.

In order to illustrate the principle of the measurement one typical streak image is displayed in the lower part of Fig. 2. It shows part of the charge-state distribution of Ar ions after passing through the discharge tube. The setting of the dipole field for this image was such that the recording range of the detector covered charge state 13 to 17. Before ignition of the discharge the charge-state distribution of the Ar ions with initial charge state 10 is determined by the 2.5 mbar of hydrogen gas in the tube. It has its maximum at charge state 12 (as recorded with a higher dipole field) with some fraction of the ions in charge state 13 and 14. This is still below the equilibrium value of about 16 which is reached at a much higher hydrogen pressure. Shortly after triggering the discharge the beam vanishes from the scintillator, an unwanted side effect which will be explained below. In the period after the pinch phase the signal appears again on the detector and one can follow the evolution of the charge-state distribution of heavy ions that have passed through the plasma as the plasma column expands. The center of the charge-state distribution is initially at charge state 16 and then moves to lower charge states with decreasing plasma density. Also the effect of the energy loss is clearly visible on the streak image. In the phase of high plasma density and corresponding high-energy loss the position of the beam spots are shifted upwards corresponding to a stronger deflection in the dipole magnet. One advantage of the chosen experimental setup is that the streak images can directly be compared to the results of the energy-loss measurement by the time-of-flight method. The dashed lines superposed on the streak image in Fig. 2 indicate the expected deflection of the ion beam as calculated from the measured energy loss. The results of the two types of measurements are in perfect agreement.

The reason for the disappearance of the beam from the detector during certain phases of the discharge is the azimuthal magnetic field caused by the high electrical current in the plasma. In a recent experiment a strong focusing of heavy-ion beams by this Z pinch device has been observed, with a minimum focal length of some 20 cm [17,18]. As a result of this feature a Z pinch represents an attractive alternative to conventional quadrupole lenses whenever pulsed focusing is required. For the charge-state measurements, however, the effect was negative because the high divergence angle of the strongly focused beam could not be accepted by the conventional beam transport system and therefore the beam vanished from the scintillator located several meters behind the plasma target.

Further analysis of the streak images is straightforward. For different time steps an effective mean charge $Z_{\mathrm{eff}}=\sum_i h_i Z_i$ is determined from the measured charge-state distribution spectrum. Correlation of this value with the plasma density at the same time yields the effective charge as a function of plasma density.

The results of the experiments are summarized in Fig. 3. It shows the effective charge of Ar ions and Xe ions as a function of plasma density. Data for two different initial charge states are displayed for each projectile.

In the case of Ar, 10+ and 15+ ions are ionized to higher charge states with increasing plasma density. A maximum is reached at $Z_{\mathrm{eff}}=16.2$ which is the equilibrium charge in plasma. We compare this result to the respective value of the Betz formula for cold gas [3] amounting to $Z_{\mathrm{eff}}^{\mathrm{cold}}=15.8\pm0.5$ (dotted line in Fig. 3). Martin and Northcliffe determined this value experimentally [19] with a result of $Z_{\mathrm{eff}}^{\mathrm{cold}}=16.2\pm0.35$, which is in good agreement with the semiempirical formula of Betz. Thus the value of the effective charge for Ar ions at 4.8 MeV/amu is equal in plasma and cold hydrogen gas. This is due to the fact that an Ar ion at charge state 16 is a very stable He-like configuration and the high binding energy of the K-shell electrons prevents further ionization in the gas and in the plasma case.

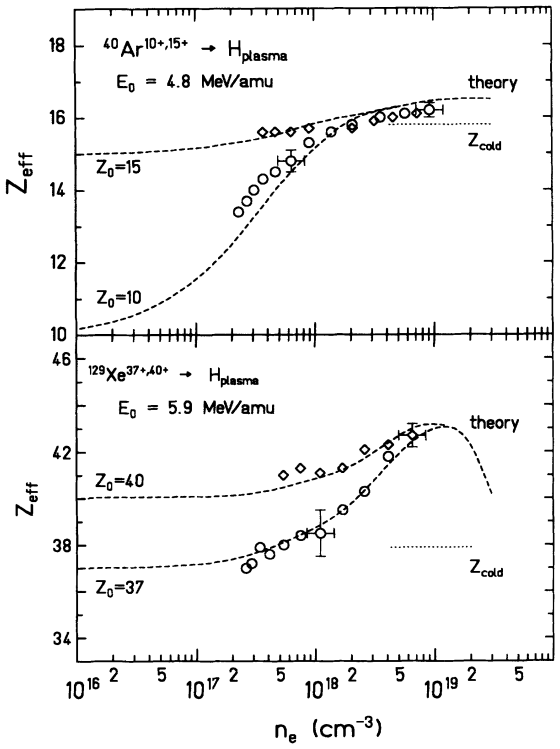

FIG. 3. Effective charge of Ar ions and Xe ions after passing through the plasma target, as function of plasma density. The data (symbols) are compared to the equilibrium effective charge in cold gas (dotted lines) and to model calculations (dashed lines).

The situation is different for Xe ions at 5.9 MeV/amu. Data for initial charge states 37 and 40 are displayed. In the plasma the effective charge increases up to $Z_{\text{eff}}=43$ which is five charge states higher than the corresponding value for cold gas, which again has been calculated with the Betz formula [4] which has a general accuracy of better than one charge state. Our data are the first experimental evidence for an enhanced effective charge of fast heavy ions in plasma.

The data are compared to the results of theoretical calculations which were computed with a Monte Carlo code developed at GSI. It is based on the work of Peter and Meyer-ter-Vehn [7] and simulates energy loss and charge exchange of arbitrary heavy ions in fully ionized hydrogen plasma. For a detailed discussion of the models for the different charge-exchange processes we refer to Ref. [7]. The processes included in our code are projectile ionization by Coulomb collisions with target ions (CCI), and ionization by free electrons (CCE), radiative electron capture (REC), and dielectronic recombination (DR). One essential point has been modified with respect to the theory of Ref. [7]. The ionization cross sections for CCI that are calculated in the binary encounter model (BEM) of Gryzinski [20,21] turn out to be too small to represent measured total electron-loss cross sections. A comparison with experimental data for electron loss of heavy ions with comparable energy in gases [22] showed that the BEM cross sections have the correct energy and charge-state dependence but on an average underestimate the data by about a factor of 2.5. This can only partly be explained by collisions with electrons which also contribute to the ionization cross section; furthermore, Auger cascades following inner-shell ionization contribute to the total electron-loss cross section. Capture of projectile electrons into protons of the hydrogen plasma is a negligible process for our experimental conditions. The larger part of the difference must be considered as a weakness of the BEM. In our code therefore all BEM cross sections are multiplied by a factor of 2.5 to simulate the total electron-loss cross section.

As can be seen, theory is in excellent agreement with the data. Not only the equilibrium charge state but also the evolution from the initial charge state to its equilibrium value are reproduced correctly, even though simple atomic models are involved in the calculations. The predictions of Refs. [5–7] are completely confirmed by the experiment.

In summary, we have measured the charge state of fast heavy ions after passing through a plasma target. For the first time an enhancement of the effective charge in plasma was demonstrated. The effect is well described by theory. It is important for the plasma production with intense heavy ion beams and may also be exploited for an efficient plasma stripper in a linear heavy-ion accelerator [8].

We are particularly grateful to R. Bock and S. Witkowski for their continuous strong support of this experiment. This work was supported by the German Federal Minister of Research and Technologie (BMFT) under Contract No. GSI 06MM660.

[1] R. C. Arnold and J. Meyer-ter-Vehn, Z. Phys. D **9**, 65 (1988).

[2] C. Deutsch, G. Maynard, R. Bimbot, D. Gardès, S. Della-Negra, M. Dumail, B. Kubica, A. Richard, C. Fleurier, A. Sanba, D. H. H. Hoffmann, K. Weyrich, and H. Wahl, Nucl. Instrum. Methods Phys. Res., Sect. A **278**, 38 (1989).

[3] H.-D. Betz, Rev. Mod. Phys. **44**, 465 (1972).

[4] H.-D. Betz, in *Applied Atomic Collision Physics,* edited by H. S. W. Massey, E. W. McDaniel, and B. Bederson, Pure and Applied Physics Vol. 43 (Academic, Orlando, 1983), Vol. 4, p. 1.

[5] E. Nardi and Z. Zinamon, Phys. Rev. Lett. **49**, 1251 (1982).

[6] Th. Peter, R. Arnold, and J. Meyer-ter-Vehn, Phys. Rev. Lett. **57**, 1859 (1986).

[7] Th. Peter and J. Meyer-ter-Vehn, Phys. Rev. A **43**, 1998 (1991); **43**, 2015 (1991).

[8] G. D. Alton, R. A. Sparrow, and R. E. Olson, Phys. Rev. A **45**, 5957 (1992).

[9] F. C. Young, D. Mosher, S. J. Stephanakis, S. A. Goldstein, and T. A. Mehlhorn, Phys. Rev. Lett. **49**, 549 (1982).

[10] J. N. Olsen, T. A. Mehlhorn, J. Maenchen, and D. J. Johnson, J. Appl. Phys. **58**, 2958 (1985).

[11] D. H. H. Hoffmann, K. Weyrich, H. Wahl, Th. Peter, J. Meyer-ter-Vehn, J. Jacoby, R. Bimbot, D. Gardès, M. F. Rivet, M. Dumail, C. Fleurier, A. Sanba, C. Deutsch, G. Maynard, R. Noll, R. Haas, R. Arnold, and S. Maurmann, Z. Phys. A **30**, 339 (1988).

[12] D. H. H. Hoffmann, K. Weyrich, H. Wahl, D. Gardès, R. Bimbot, and C. Fleurier, Phys. Rev. A **42**, 2313 (1990).

[13] K.-G. Dietrich, D. H. H. Hoffmann, H. Wahl, C. R. Haas, H. Kunze, W. Brandenburg, and R. Noll, Z. Phys. D **16**, 229 (1990).

[14] K.-G. Dietrich, K. Mahrt-Olt, J. Jacoby, E. Boggasch, M. Winkler, B. Heimrich, and D. H. H. Hoffmann, Laser Part. Beams **8**, 583 (1990).

[15] R. Noll, H. Kunze, and C. R. Haas, Nucl. Instrum. Methods Phys. Res., Sect. A **278**, 85 (1989).

[16] H. Kunze, R. Noll, C. R. Haas, M. Elfers, J. Hertzberg, and G. Herziger, Laser Part. Beams **8**, 595 (1990).

[17] E. Boggasch, J. Jacoby, H. Wahl, K.-G. Dietrich, D. H. H. Hoffmann, W. Laux, M. Elfers, C. R. Haas, V. P. Dubenkov, and A. A. Golubev, Phys. Rev. Lett. **66**, 1705 (1991).

[18] M. Elfers, C. R. Haas, E. Boggasch, K.-G. Dietrich, D. H. H. Hoffmann, R. Noll, H. Kunze, and G. Herziger, Z. Phys. D **18**, 207 (1991).

[19] F. W. Martin and L. C. Northcliffe, Phys. Rev. **128**, 1166 (1962).

[20] M. Gryzinski, Phys. Rev. **138**, A305 (1965); **138**, A322 (1965); **138**, A336 (1965).

[21] J. H. McGuire and P. Richard, Phys. Rev. A **8**, 1374 (1973).

[22] W. Erb, GSI Report No. P-7-78, 1978 (unpublished).

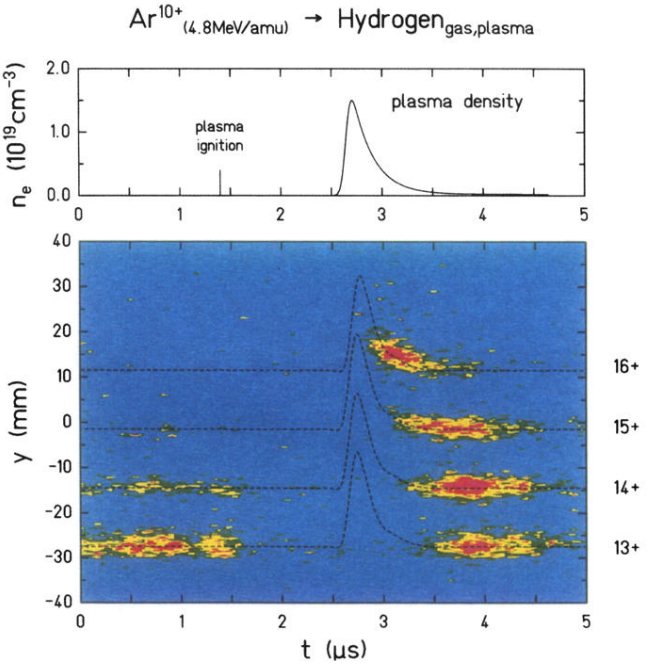

FIG. 2. Plasma density on the beam axis vs time (top) and streak image of the charge-state distribution of Ar ions after passing through the plasma target (false color image, bottom).